Acta Cryst. (1976). A32, 513

International Union of Crystallography

Commission on Spin, Charge and Momentum Density.

Project No. 1. Standardization of Compton Profile Measurements – The Compton Profile of Water

Project Coordinator: BRIAN G. WILLIAMS, *Department of Applied Physics, University of Strathclyde, Glasgow, G4 0NG, Scotland.* Contributors: JOSHUA FELSTEINER, VESA HALONEN, TIMO PAAKKARI, SEPPO MANNINEN, WILLIAM REED, PETER EISENBERGER, RICHARD WEISS, PHILIP PATTISON, MALCOLM COOPER

(*Received* 9 *July* 1975; *accepted* 27 *October* 1975)

Thirteen measurements of the Compton profile of water carried out in five different laboratories are compared. The possible sources of error inherent in Compton measurements are analysed. Inconsistent normalization of the various profiles is found to be an important source of error. After renormalization of the profiles the results are found to be consistent to within ±2% of the peak height of the profiles. It is shown that all probable sources of error can be analysed in terms of five general types of error and further that the effects of all of these types of error on the shape of the Compton profile are almost indistinguishable from one another. The determination of the position of the Compton peak is found to be another important potential source of error in experimental measurements. Certain assumptions relating to the conversion to a momentum scale were found to be mistaken and are corrected. A comparison of currently accepted relativistic and non-relativistic expressions for the cross section revealed that they are not in fact significantly different. Multiple scattering is found to be the only major source of error which is not yet well understood. Each experimental measurement is assessed in detail with particular regard to the differences between the techniques used by the contributing groups. Proposals are made relating to the accumulation, processing and presentation of Compton data. It is concluded that a reproducibility of ±1% of the peak height of the profile is quite feasible and that in a differential experiment ±0·5% or even better is possible.

1. Introduction

One of the problems inherent in all experimental work lies in determining the extent to which systematic errors, arising either from the data processing procedures or from the actual experimental technique, affect the results. Probably the most fruitful approach to such problems is for a number of independent research groups to carry out essentially the same experiment and then to compare the results. Projects of this nature have already been carried out in relation to X-ray diffraction measurements (Abrahams *et al.*, 1967; Mackenzie & Maslen, 1968; Abrahams, Hamilton & Mathieson, 1970; Paakkari, Suortti & Inkinen, 1970). As a result of these projects considerable insight has been obtained concerning both the reliability and reproducibility of X-ray diffraction measurements.

Interest in the Compton effect as a tool for the determination of electron momentum distributions has grown rapidly over the last ten years. As recently as 1965 there were only two laboratories undertaking systematic measurements of Compton profiles. Since then, six more groups have begun to carry out measurements in this field and at least five other groups are regularly reporting results of theoretical calculations of Compton profiles. With this in mind, it was decided that a project along the lines of the diffraction projects should be carried out with a view to estimating the reliability of Compton scattering data. As well as testing the limits of accuracy of Compton measurements, it is hoped that one of the end products of this project will be a reference profile which workers involved in setting up Compton scattering units will be able to use as a standard by which to judge their results.

In this report it will be assumed that the reader is familiar with the experimental techniques involved in the measurement of X-ray and γ-ray Compton profiles. For details of the X-ray technique the reader is referred to the review article by Cooper (1971) and for details of the γ-ray technique to the paper by Eisenberger & Reed (1972). A good general review is given by Epstein (1975).

2. Participants

All the research groups currently known to be involved in Compton profile measurements were invited to participate in the project. The following people agreed to carry out a measurement using the radiations indicated –

Felsteiner, J – Am
Hosoya, S. – Am
Halonen, V. – Mo
Loupias, G. – Mo
Manninen, S. and Paakkari, T. – Am
Pattison, P., Cooper, M. J. and Williams, B. G. – Mo, Am
Reed, W. A. and Eisenberger, P. – Te
Schulke, W. – ?
Weiss, R. J. – Ag.

[Am indicates 59·54 keV γ-rays from a ^{241}Am source, Te indicates 159 keV γ-rays from a ^{123m}Te source, Mo indicates 17 keV (0·71 Å) Mo $K\alpha$ fluorescence X-rays and Ag indicates 22 keV (0·53 Å) Ag $K\alpha$ fluorescence X-rays.]

Measurements have been received from Felsteiner, Halonen, Paakkari and Manninen, Reed and Eisenberger, Weiss, and Pattison.

3. Preliminary planning

The single most important decision in planning the project lay in deciding what sample to use. Indeed, before choosing the actual substance it was necessary to decide whether to supply each participant with a sample, in which case a preliminary check could be carried out to ensure that the samples were all effectively identical, or whether to let individual groups prepare their own sample of some standard material. Since the latter course of action was

closer to the usual experimental situation, it was decided that each group should prepare their own sample. The choice of what substance to use for the sample was then limited by the following considerations.

Most important of all it had to be a material which gives a reasonably high intensity for both X-ray and γ-ray experiments. This meant that only elements of atomic number less than about 10 could be considered.

Secondly, it had to be easy to prepare in a pure and reproducible state so that there would be no significant difference between samples.

Thirdly, there should be no anisotropy in the samples so that the sample orientation would not affect the results.

Finally, the sample should be of such a nature that reasonably accurate theoretical profiles are available for comparison with the eventual experimental best estimate. (This last consideration is of secondary importance since the prime aim of the project is to carry out an inter-experimental comparison.)

As a result of these considerations three possible samples were considered – helium, water and graphite. The main advantage of helium is that very accurate theoretical profiles are available (Eisenberger & Reed, 1972) but the difficulties of containing the sample were felt to outweigh this. The advantage of graphite was that, being a solid, no container would be required but here the problem of preparing identical samples arises since there appears to be a significant degree of anisotropy in graphite (Reed, Eisenberger Pandey & Snyder, 1974) and the existence of varying degrees of preferred orientation could ruin the entire project. This left water, which satisfies all the criteria listed above except that some form of container is required. Nevertheless, provided careful measurements of the contribution from the container are made there should be no difficulty in subtracting this as background. To standardize the sample geometry to some extent it was suggested that the sample container be made of a ring of some suitable material such as brass with thin mylar windows glued to the front and back. Since the Compton profile of the carbon in the plastic should be reasonably similar to the Compton profile of water, any error in subtracting the background should be minimized.

Having decided on the sample then, the laboratories mentioned above were asked to carry out a measurement on the Compton profile of water.*

4. Data and experimental results

The Compton profiles submitted by the various participants are given in Table 1. Each data set is specified by a number and where more than one set of data has been submitted the subsets are specified by the letters *A*, *B*, *C*, and so on.* Included in Table 1 is a near Hartree–Fock (NHF) profile (Tanner & Epstein, 1974). However, it should be stressed that no special significance should be attached to differences between this and the various experimental profiles at this stage of the project, since until the inter-experimental comparison is finalized a comparison with theory is of little significance.

* Precise details of the information required and the experimental details of each set of data received have been deposited with the British Library Lending Division as Supplementary Publication No. SUP 31498 (18 pp., 1 microfiche). Copies may be obtained through The Executive Secretary, International Union of Crystallography, 13 White Friars, Chester CH1 1NZ, England.

Table 1. *Experimental Compton profiles of water*

The momentum p is in atomic units. The profiles are normalized to the NHF profile between 0 and 4 a.u. The last row gives the sample thickness in cm. The radiations used were as follows: set 1 – Ag $K\alpha$, 2 – Am, 3 – Te, 4 – Am, 5 – Mo $K\alpha$.

P	NHF	1A	2A	2B	2C	2D	3A	3B	4A	4B	4C	4D	5A	5B	MEAN
.0	3.794	3.622	3.497	3.551	3.574	3.617	3.664	3.691	3.553	3.626	3.642	3.734	3.725	3.779	3.689
.1	3.775	3.612	3.438	3.423	3.539	3.579	3.644	3.678	3.526	3.595	3.617	3.716	3.698	3.740	3.663
.2	3.717	3.530	3.356	3.376	3.476	3.521	3.583	3.615	3.461	3.524	3.548	3.651	3.612	3.650	3.593
.3	3.614	3.449	3.270	3.327	3.335	3.376	3.484	3.522	3.360	3.418	3.439	3.538	3.514	3.492	3.475
.4	3.462	3.296	3.182	3.151	3.207	3.203	3.346	3.387	3.225	3.280	3.292	3.379	3.371	3.365	3.326
.5	3.261	3.154	3.007	3.005	3.053	3.067	3.170	3.208	3.059	3.107	3.113	3.177	3.166	3.181	3.157
.6	3.021	2.950	2.804	2.832	2.837	2.856	2.960	2.991	2.866	2.904	2.908	2.940	2.925	2.966	2.941
.7	2.753	2.716	2.584	2.620	2.594	2.608	2.721	2.741	2.651	2.679	2.681	2.686	2.677	2.717	2.694
.8	2.473	2.472	2.378	2.350	2.418	2.422	2.463	2.473	2.420	2.437	2.441	2.426	2.442	2.444	2.447
.9	2.194	2.238	2.122	2.088	2.149	2.145	2.198	2.201	2.180	2.187	2.195	2.166	2.191	2.170	2.184
1.0	1.928	1.984	1.903	1.951	1.869	1.874	1.940	1.938	1.942	1.939	1.950	1.916	1.927	1.912	1.925
1.2	1.460	1.526	1.491	1.476	1.490	1.484	1.479	1.473	1.502	1.487	1.494	1.470	1.451	1.454	1.482
1.4	1.096	1.158	1.164	1.137	1.151	1.137	1.119	1.111	1.144	1.118	1.120	1.112	1.128	1.124	1.127
1.6	.827	.875	.927	.934	.873	.857	.859	.847	.886	.852	.849	.845	.885	.872	.859
1.8	.637	.661	.763	.756	.718	.702	.677	.661	.711	.681	.691	.651	.695	.653	.666
2.0	.503	.549	.627	.620	.620	.616	.549	.533	.589	.569	.555	.523	.570	.563	.557
2.5	.316	.356	.429	.430	.414	.410	.355	.346	.391	.383	.372	.355	.343	.348	.363
3.0	.226	.244	.300	.293	.283	.275	.249	.243	.284	.274	.266	.256	.249	.241	.252
3.5	.182	.183	.224	.226	.221	.219	.188	.182	.210	.202	.203	.197	.176	.175	.191
4.0	.138	.142	.174	.171	.161	.156	.148	.145	.165	.163	.156	.151	.132	.136	.146
5.0	.089	.000	.106	.105	.105	.104	.092	.091	.105	.101	.103	.090	.086	.089	.094
6.0	.059	.000	.000	.000	.000	.000	.060	.060	.068	.065	.066	.072	.057	.058	.063
7.0	.039	.000	.000	.000	.000	.000	.039	.039	.045	.044	.042	.050	.036	.041	.043
8.0	.026	.000	.000	.000	.000	.000	.026	.025	.000	.000	.000	.000	.000	.000	.025
9.0	.017	.000	.000	.000	.000	.000	.017	.015	.000	.000	.000	.000	.000	.000	.015
10.0	.012	.000	.000	.000	.000	.000	.011	.011	.000	.000	.000	.000	.000	.000	.011
15.0	.002	.000	.000	.000	.000	.000	.002	.004	.000	.000	.000	.000	.000	.000	.004
20.0	.001	.000	.000	.000	.000	.000	.000	.000	.000	.000	.000	.000	.000	.000	.000
.0	.000	.150	3.000	2.000	1.000	.000	.600	.300	1.000	.600	.300	.100	2.000	.300	.000

5. Preliminary comparison of results

From data sets 2 to 5, for which measurements were carried out on samples of more than one thickness, it is apparent that the measured Compton profile depends on the sample thickness. Since this variation with thickness is assumed to arise from the presence of multiple scattering in the data the logical step appears to be to extrapolate to zero thickness (Reed & Eisenberger, 1972; Manninen, Paakkari & Kajantie, 1974). However, it is not clear just how one should do the extrapolation, if indeed an extrapolation can be done at all, and so for this first comparison only the thinnest samples from each data set were used. A more detailed discussion of the dependence of the profile shape on multiple scattering and sample thickness is given in § 7·7 below.

Before the comparison is made, several points should be noted. The first is that the different groups used different criteria for the normalization of their profiles. Data set 1 was normalized so that the area from 0 to 4 a.u. was equal to the Hartree–Fock free-atom value, set 2 so that the area from 0 to 5 a.u. was equal to 5 e, set 3 so that the area from 0 to 15 a.u. was equal to 5 e and sets 4 and 5 so that the area from 0 to 7 a.u. was equal to the Hartree–Fock free-atom value. In order to make a meaningful comparison of the data it was necessary to renormalize the data using the same criterion for each set. The criterion adopted was that they should all have the same area as the near-Hartree–Fock (NHF) profile given in Table 1, between 0 and 4 a.u., namely 4·682 e. (The data in Table 1 are the data as received from the various participants but renormalized in this way). To make the importance of this renormalization clear, Table 2 gives the percentage change in $J(0)$ for each set of data as a result of this renormalization. Since these changes (up to 4%) are of the same order as the differences between the data sets the renormalization is clearly of crucial importance.

Table 2. *Percentage change in the value of $J(0)$ due to renormalization of the profiles*

Data set	1	2	3	4	5
$\Delta J(0)$ %	1·7	−3·5	0·0	0·5	0·8

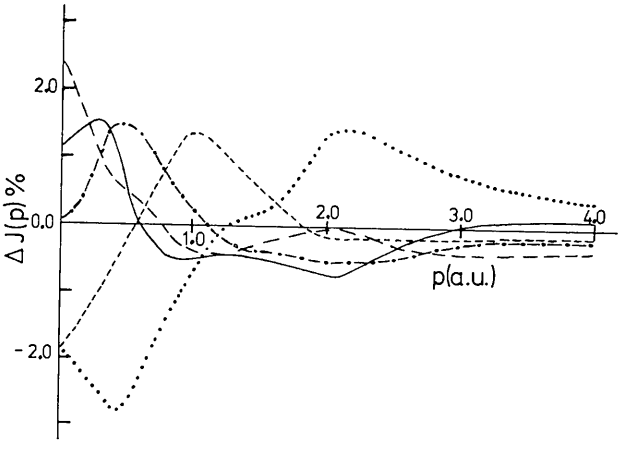

Fig. 1. Differences between individual profiles and the mean given in Table 3. The differences are plotted as a percentage of the peak height of the NHF profile. Data sets 1 --------; 2 ··········; 3 -·-·-·-·-·-; 4 ————; 5— — — —.

The second point to be noted is that for data set 2 no absorption correction was applied on the grounds that if the data is extrapolated to zero thickness no absorption correction is necessary. For this reason the data for set 2 was extrapolated to zero thickness. Further discussion of this will be given in § 7·7 below.

Since the differences between the sets of data are fairly small it is necessary to present the data as differences from some profile and in Fig. 1 the difference is plotted between each data set and the mean. In order to get a sense of proportion into the data the differences are plotted as a percentage of the *peak height* of the NHF profile given in Table 1, namely 3·794.

At this stage of the data analysis it should be noted that no special significance should be attached to the mean. The only feature of interest is the difference between pairs of profiles. However, since some profile must be used as a base so that the individual measurements can be expressed as differences from this base, the mean is the most convenient to use.

From the numerical values given in Table 3 and the corresponding plots in Fig. 1, it can be seen that the total spread of the results is about ±2% at zero momentum and about ±0·5% at $p=4$ a.u. This is not far outside the quoted experimental errors which range from ±1% to ±1·5% at $p=0$ a.u. and from ±0·2% to ±0·3% at $p=4$ a.u. It should be noted that the curves plotted in Fig. 1 were slightly smoothed when drawn to avoid the figure becoming an unintelligible jumble of lines. Nevertheless, none of the data points are more than about 0·4% from the curves and most are within about 0·2% of the curves. From Fig. 1 it appears that three of the curves (data sets 3, 4 and 5) are particularly close to one another, that one of the X-ray experiments (data set 1) is somewhat wider than these three

Table 3. *Differences between individual profiles and the mean given in the last column* (%)

All quantities are multiplied by a factor of 10^3.

p(a.u.)	NHF−M	1−M	2−M	3−M	4−M	5−M	M
0	2779	−1759	−1882	58	1195	2388	3689
100	2949	−1356	−2225	177	1390	2014	3663
200	3258	−1664	−1910	566	1508	1500	3593
300	3657	−696	−2627	1231	1658	433	3475
400	3584	−784	−3235	1611	1386	1022	3326
500	2731	−94	−2393	1342	512	632	3157
600	2119	258	−2235	1318	−17	676	2941
700	1560	595	−2250	1240	−206	622	2694
800	675	654	−677	680	−563	−95	2447
900	256	1422	−1023	453	−480	−372	2184
1000	83	1556	−1339	341	−229	−328	1925
1200	−572	1169	67	−221	−295	−720	1482
1400	−809	604	265	−421	−384	−65	1127
1600	−850	414	−68	−322	−371	348	859
1800	−759	−119	946	−120	−379	−329	666
2000	−1422	−200	1556	−621	−897	162	557
2500	−1239	−183	1240	−459	−202	−396	363
3000	−680	−201	619	−239	109	−287	252
3500	−246	−216	742	−251	143	−418	191
4000	−209	−92	264	−28	122	−266	146
5000	−121		273	−71	−86	−115	94
6000	−112			−87	238	−151	63
7000	−112			−114	182	−69	43
8000	27			0			25
9000	53			0			15
10000	27			0			11
15000	−53			0			4
20000	26			0			0

Table 3. (*cont.*)

Quoted experimental errors expressed as a percentage of the peak height of the profiles

p (a.u.)	1	2	3	4	5
0·0		1·5	1·0	1·0	
0·5		1·4	0·9	1·0	
1·0		1·3	0·8	0·8	
2·0		0·8	0·3	0·3	
4·0		0·3	0·2	0·2	
7·0		—	—	0·1	
10·0			0·2		

and that one of the γ-ray measurements (data set 2) is much wider still. [Note that a 'wide' curve will give a low value of $J(0)$].

From this preliminary examination it seems that all of the Compton scattering experiments are in reasonable agreement, but there seems to be a significant difference between two of the profiles and the remaining three.

Having made this initial comparison then, the rest of this report will be devoted to a consideration of the following two questions. First of all, is it possible to trace the residual discrepancies and thus either improve the agreement or make an estimate as to which of the profiles is likely to be nearer to the 'true' profile? Secondly, is it possible to decide if there is likely to be any significant, common, but undetected, systematic error which would cause all the experiments to be in error by the same amount?

6. The effect of systematic errors

When Compton measurements are carried out, the possible systematic errors may be divided into two classes. The first involves errors in the raw data. For example, an incorrect determination of the scattering angle will lead to an error in the estimated position of the peak of the profile and hence the zero of the momentum scale. The second involves errors in the data processing. For example, the expression used to calculate the wavelength dependence of the absorption in the sample may be incorrect leading to a systematic error in the intensity as a function of momentum. However, to a reasonable degree of accuracy, all probable errors may be written in one of the following forms. [$J(p)$ is the 'correct' profile and $J'(p)$ the profile with the error.]

$$\begin{array}{lll} (1)\ \text{Linear error} & J'(p)=(1+\lambda p)J(p) & \\ (2)\ \text{Scale error} & J'(p)=J[(1+\sigma)p] & \\ (3)\ \text{Shift error} & J'(p)=J(\pi+p) & (1) \\ (4)\ \text{Background error} & J'(p)=J(p)+\beta J(0) & \\ (5)\ \text{Convolution error} & J'(p)=J(p)*R(p,\gamma) & \end{array}$$

where λ, σ, π and β are small constants and $R(p,\gamma)$ is an apparatus function of width γ. In order to obtain an estimate of the effect of the errors, each of them was applied to the NHF profile given in Table 1. The 'error' profiles were then renormalized to have the same area as the original profile in the range 0 to 4 a.u. and Table 4 gives the difference between the original profile and the 'error' profile for suitable values of the parameters. From Table 4 it can be seen that the change in the profile is almost linear with respect to each parameter in the range under consideration. More precisely $J'(p)$–$J(p)$ varies linearly with each of the error parameters given above provided $J'(p)$ is renormalized to have the same area as $J(p)$. Since the error was greatest at $p=0$ in each case, the value of each parameter required to produce a 1% change in $J(0)$ was calculated and the values recorded in Table 5. Also for later reference, Fig. 2 gives difference plots for each type of error. From Table 5

Table 4. *The effect of various errors on the NHF Compton profile of water*

The parameters are defined in the text. The table gives the difference between each 'error' profile and the original profile as a percentage of $J(0)\times 10^2$ after the area between 0 and 4 a.u. has been renormalized.

	Linear $\lambda\times10^3=$ (a.u.$^{-1}$)		Scale $\sigma\times10^3=$		Peak shift $\pi\times10^3=$ (a.u.)		Background $\beta\times10^3=$		Convolution $\gamma\times10^3=$ (a.u.)	
p (a.u.)	−10	10	−10	10	−10	10	−5	5	150	300
0·0	92	−90	−99	78	−87	70	114	−110	−47	−116
0·1	82	−80	−98	77	−76	59	113	−109	−48	−120
0·2	70	−69	−94	71	−65	46	111	−107	−52	−129
0·3	59	−58	−87	62	−51	31	106	−103	−54	−135
0·4	47	−46	−75	50	−35	15	99	−96	−53	−131
0·5	36	−35	−59	35	−18	1	91	−88	−45	−111
0·6	25	−25	−42	19	−2	−11	80	−78	−35	−83
0·7	16	−15	−23	4	11	−20	69	−67	−22	−48
0·8	7	−7	−6	−9	20	−25	57	−55	−11	−15
0·9	1	−1	8	−19	26	−27	44	−43	−1	16
1·0	−4	4	19	−23	28	−24	33	−32	12	39
1·2	−11	11	35	−28	30	−19	13	−12	27	66
1·4	−14	14	38	−28	24	−14	−3	3	26	63
1·6	−15	15	34	−23	17	−9	−15	14	22	53
1·8	−15	15	28	−19	11	−5	−23	22	16	39
2·0	−15	14	22	−10	7	0	−29	28	17	38
2·5	−13	13	16	−5	3	1	−37	36	11	24
3·0	−13	12	0	−2	−0	2	−41	40	5	11
3·5	−13	12	3	−4	−2	1	−43	42	−1	−1
4·0	−11	11	6	−2	−1	1	−45	43	2	4
5·0	−10	10	4	−0	−1	1	−47	45	2	4
10·0	−3	3	4	−0	0	0	−50	49	1	0
15·0	−1	1	1	−0	0	0	−51	49	0	0
20·0	−1	0	0	0	−0	0	−51	49	0	0

it can be seen for example that a linear error of 0·011 a.u.$^{-1}$ will cause a 1% error in $J(0)$. Similarly, an error in converting to a p_z scale of 1%, an error in the position of the Compton peak of 0·013 a.u. or an error in the background of 0·5% of the peak height will all cause an error of 1% in $J(0)$. Each of these types of error will be discussed in relation to the experimental measurements below. However, it is immediately clear from the similarity in the shapes of the difference curves plotted in Fig. 2 that it will be virtually impossible, on the basis of the final data alone, to attribute a systematic error in a difference plot to any one of these types of error. The only type of error which may be distinguishable from the others is the background error which is quite large at high values of q by comparison with the others. A particularly important feature to note is that the presence of a 'linear' error or a 'shift' error will destroy the symmetry of the Compton profile about $p=0$. The symmetry of the final profile can therefore be used as a check on these types of error. Alternatively, if the mean of the two sides of the profile is used, these errors should cancel. (This assumes, of course, that the impulse approximation is valid and that there is no interference from binding effects in the region of interest.)

Table 5. *Values of the error parameters (defined in the text) which will give rise to a* 1% *error in* $J(0)$

$\lambda = +0{\cdot}011$ a.u.$^{-1}$
$\sigma = -0{\cdot}011$
$\pi = -0{\cdot}013$ a.u.
$\beta = 0{\cdot}0045$
$\gamma = 0{\cdot}3$ a.u. (Gaussian, FWHM)

7. Discussion of error sources

In order to carry out a thorough analysis of the error sources in a Compton experiment it is necessary to go through the rather tedious procedure of examining each step in the analysis of Compton scattering data and try to get some idea of the effect each step is likely to have on the final result. To keep things clear the whole procedure is set out in Table 6. The order of the corrections is not necessarily correct but is the order in which they are usually considered.

As shown in Table 6, a generalized Compton experiment uses a monochromatic beam of photons as the probing radiation. The photons are then scattered from the electrons in a suitable sample and the energy (or wavelength) shift of the photons scattered through a fixed angle is observed. In short, the experiment measures the probability that a photon leaves a radiation source with some fixed momentum, is scattered within the sample and is registered in a detector sensitive only to photons with some other well defined momentum. In this project, measurements of this energy distribution have been carried out using both the X-ray and the γ-ray techniques. Therefore the first thing to be borne in mind is the possibility of detecting systematic errors which are likely to be different for the two types of experiment. The second thing to remember is that the incident photon energies used in different experiments cover a wide range (~20 keV for data sets 1 and 5, 60 keV for sets 2 and 4 and 160 keV for set 3), so that the possibility exists of detecting systematic errors which are strongly energy dependent.

The possible error sources are then as follows.

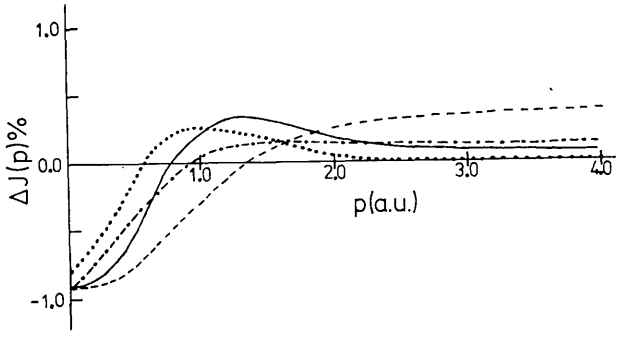

Fig. 2. The effect of various errors on the NHF profile of water. The curves are the linear part of the corrections in Table 5. -·-·-·- Linear error, $\lambda=0{\cdot}01$ a.u.$^{-1}$; ——— Scale error, $\sigma=-0{\cdot}01$; ····· Shift error, $\pi=-0{\cdot}01$ a.u.; – – – – Background error, $\beta=0{\cdot}004$.

Table 6. *Experiment*

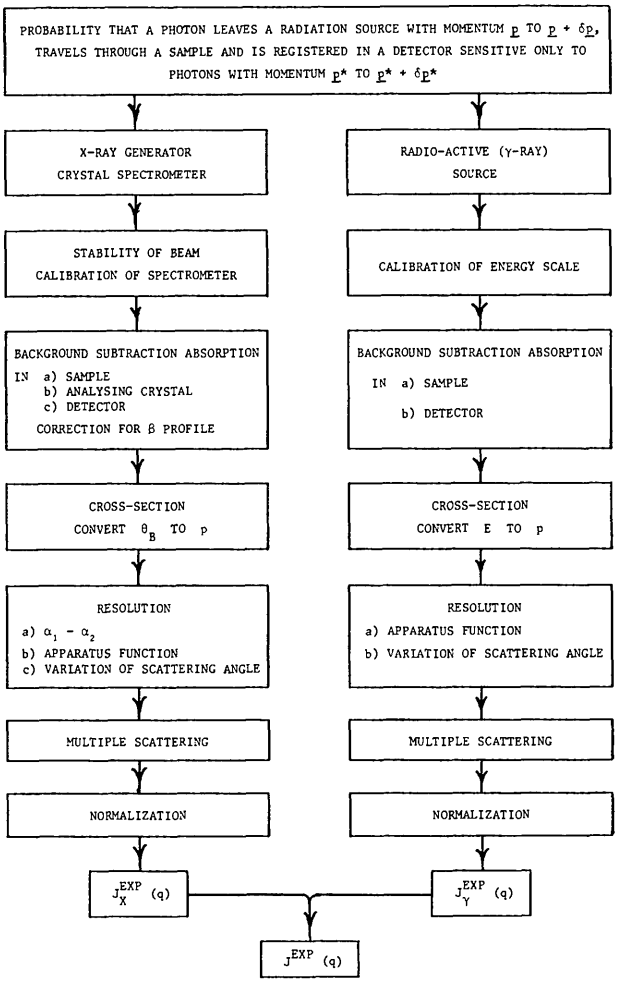

7.1 *Reliability of the apparatus*

The first thing to be considered is the reliability of the apparatus.

In the X-ray experiments this means that the intensity of the incident beam should be stable to within about 0·2% (if the random errors are to be of the order of 0·5%), and also that the spectrometer is correctly calibrated so that the conversion from Bragg angle to wavelength is correct. The beam stability can be checked by carrying out a series of measurements over the same part of the profile which can then be tested for consistency. Both short-term and long-term fluctuations should be considered since a test for one might easily overlook the other. The spectrometer calibration is easily verified by measuring the Bragg angles of standard fluorescent wavelengths. In order to estimate the accuracy with which the Bragg angle should be determined, the error in the peak shift for a given error in the Bragg angle has been calculated (Appendix I). From this calculation it follows that the error is almost independent of the scattering angle in the region of interest. Further, to ensure that the error in $J(0)$ is not more than 0·2%, the Bragg angle corresponding to the peak shift should be determined to whithin 0·001° of 2θ. This is within the limits on most X-ray spectrometers and should not give rise to any difficulty. Further, as shown in Table 5, it can be seen that with the peak position fixed, the error in the Bragg angles as measured with respect to the Compton peak should be no more than 0·2%, but again this should present no problem with most X-ray spectrometers.

In the γ-ray experiments the beam stability is immaterial since the detector observes the whole spectrum simultaneously. It is necessary, however, to ensure that the energy scale is correctly calibrated, but this is easily done by observing the energies of the radiation from standard γ-ray sources. At high angles the error in the peak shift is almost independent of the scattering angle and it is shown in Appendix I that the energy corresponding to the peak shift should be determined to within 24 eV for Te γ-rays and 12 eV for Am γ-rays. This is within the limits of most solid-state detecting systems. As in the X-ray case, the energy should be determined with respect to the Compton peak to an accuracy of at least 0·2%.

7.2 *Background subtraction*

In the X-ray experiments there is always a lot of Bremsstrahlung radiation so that the background subtraction is quite difficult. Indeed, the signal-to-noise ratio is usually of the order of about five to one at the peak of the profile and in the tails, where the background may be considerably greater than the profile itself, it becomes virtually impossible to obtain an accurate estimate of the true curve. When subtracting the background from the X-ray data, the long-wavelength background may be in error if the points are not taken sufficiently far out in the tail to ensure that the Compton profile is effectively zero. As can be seen from Table 5, an error in the background of 0·5% of the peak height of the profile will give rise to an error of 1% in the value of $J(0)$ if the profile is renormalized between 0 and 4 a.u. of momentum. Using the NHF values of $J(q)$ in Table 1, it therefore follows that in order to ensure that the error in $J(0)$ is no more than 0·2% the background should be measured at points in the profile corresponding to at least 10 a.u. of momentum. Subtracting the background on the short-wavelength side of the $K\alpha$ lines is hindered by the presence of the $K\beta$ Compton profile so that the background points should be measured to the short-wavelength side of the $K\beta$ line. This in turn assumes that the background is flat over this rather large range of wavelength.

Fortunately, the background subtraction is quite straightforward in the γ-ray experiments since the signal-to-noise ratio is usually of the order of 500 to 1 or better. The γ-ray results should therefore provide a useful check of the tails of the X-ray results.

With both techniques it is of course necessary to take into account the possibility of Compton scattering from the air and the windows of the scattering chamber, but careful measurements of the intensity from the empty sample holder should provide a reasonable estimate of this.

7.3 *Energy dependence of absorption*

The next step in the processing of Compton scattering data arises from the fact that the scattered photons have a range of different energies or wavelengths so that the absorption of the photons in the sample and the detecting system will vary across the profile. In both systems it is necessary to correct for the energy dependence of the absorption in the sample and in the detector and in the X-ray system it is also necessary to allow for the wavelength dependence of the absorption in the analysing crystal of the spectrometer. Here the large range of incident energies is useful since the absorption corrections vary considerably between the two systems. Since the effect of absorption in the sample is much greater for the X-rays than for the γ-rays, the latter again provide a useful check on the former. In particular, however, the correction is positive on one side of the profile and negative on the other so that, as was pointed out in § 7, the processed profiles can be checked by testing the symmetry of the final profile.

For the X-ray results it should of course be borne in mind that the tail of the $K\beta$ profile may overlap the short-wavelength side of the $K\alpha$ profile and a suitable correction will be necessary.

7.4 *Conversion to a momentum scale*

At this stage of the data processing it is usual to convert the Bragg angles or energies to momentum units. There is no essential difficulty here since, within the limitations of the impulse approximation, an exact expression can easily be derived (Viegele, Tracy & Henry, 1969). However, in the past some workers have used the simpler expression for X-ray results which follows when the change in wavelength is very much less than the initial wavelength (Cooper, 1971). If this is compared with the 'exact' result, it will be found that even for typical X-ray wavelengths this leads to a scale change of the order of 3% and hence an error of about 3% in the renormalized value of $J(0)$ (see Table 5).

Converting the results to a momentum scale assumes of course that the original parameters are measured with sufficient accuracy. In both the X-ray and the γ-ray experiments the scattering angle must be determined, to obtain both the zero and the width of the momentum scale. In Table 7 the error in the peak shift for a given error in the scattering angles is shown as a function of scattering angles and incident energies (see Appendix I). From Table 7 it can be seen that if the scattering angle is 160°, then in order to ensure that the error in $J(0)$ is no greater than 0·2% say, the scattering angle should be determined to an accuracy of at least 0·02° for Te γ-rays, 0·04° for Am γ-rays and 0·15° for Mo and Ag $K\alpha$ X-rays. At lower scattering angles an even more rigorous determination of the scattering angle is required, but conversely the requirements can be relaxed for higher scattering angles. Again, however, the error on the low-energy side and the error on the high-energy side

will be equal but of opposite sign so that the symmetry of the final profile can be used as a check.

Table 7. *Error in the peak shift due to an error in the scattering angle* (a.u./°) *for a range of incident photon energies and scattering angles*

E_0 (keV)	150°	160°	170°
160	0·150	0·100	0·050
60	0·065	0·044	0·022
20	0·023	0·016	0·008

As well as causing an error in the peak shift, an incorrect scattering angle will cause an error in the width of the momentum scale. From Table 8 it can be seen that at 160° say, the scattering angle should be determined to within about 3° if the error in $J(0)$ is to be less than 0·2% so that the error introduced in this case is less than in the previous case.

Table 8. *Error in the momentum scale due to an error in the scattering angle* (φ)

φ	Error (%/°)
150°	0·1
160°	0·07
170°	0·03

7.5 *Correction for the cross section and non-linearity of the momentum scale*

The correction for the cross section arises because the scattering cross section depends on the energy of the incident and scattered radiation as well as the momentum of the scattering electron (Manninen, Paakkari & Kajantie, 1974). However, as is shown in Appendix II, if the scattering angle is 180° the momentum dependence of the scattering cross section is approximately $1-0{\cdot}007p$ for all incident energies (with p in a.u.).

A similar correction, which affects some of the data discussed in this report, has caused confusion in the literature. It has been suggested that since the conversion from energy (of the scattered photon) to momentum (of the scattering electron) is not linear [Appendix I, equation (A1)] the correct expression for calculating the Compton profile as a function of momentum, $J(p)$, from the profile as a function of energy, $J(\omega)$, is

$$J(p)=J(\omega)\,(\partial\omega/\partial p)\,.$$

Now while this is undoubtedly true, the factor $(\partial\omega/\partial p)$ is already included in the standard expression for the cross section. [See, for example, Eisenberger & Reed (1974) equation (10). The factor $\partial\omega/\partial p$ arises in this paper from the integration over the energy conservation delta-function.] In the X-ray case, however, it is necessary to convert the Bragg angles to energy and hence momentum. The correct expression for this conversion is

$$J(\omega)=J(2\theta)\,(\partial 2\theta/\partial\omega)$$

and this factor of $(\partial 2\theta/\partial\omega)$ must be included. In Appendix II it is shown that at 180° this correction is approximately $1+0{\cdot}025p$ for Mo and Ag X-rays with LiF analysing crystal in the 400 reflexion, with p in a.u.

Both of the corrections discussed above will of course depend on the scattering angle and should be calculated separately for each case. Since the corrections vary linearly with the momentum p, errors in these corrections will destroy the symmetry of the final profile.

7.6 *Correction for the instrument function*

The next correction to be applied to the data involves deconvolution to allow for the finite resolution of the instrument function. In the X-ray experiments the instrument function has three component parts. There is the part which would usually be called the apparatus function of the spectrometer arising from the finite divergence of the Soller slits and the mosaic spread of the analysing crystal. This is easily measured by carrying out a spectral analysis of the $K\alpha$ fluorescence from the X-ray tube. There is the broadening due to the divergence of the incident beam which must be calculated from the scattering geometry and finally there is the broadening due to the use of an α doublet, the separation of which is readily obtained from standard tables. In the γ-ray experiments only the first two components are present. The 'apparatus function' is easily measured using standard γ-ray sources and the incident-beam divergence function must again be calculated.

In order to specify the total instrument function, the most suitable single parameter is probably (Epstein & Williams, 1973)

$$\text{Resolution } T^2=\text{Resolution } 1^2 + \text{Resolution } 2^2+(\tfrac{2}{9})\ \text{Resolution } 3^2$$

where 'Resolution 1^2' is the variance of the apparatus function, 'Resolution 2^2' is the variance of the effective incident beam divergence function and 'Resolution 3' is the separation of the $K\alpha$ doublet in atomic units of momentum. Typical values for the total instrument function width are 0·3 to 0·4 a.u. for X-ray experiments and 0·4 to 0·8 a.u. for γ-ray experiments (Epstein & Williams, 1973).

It is difficult to make general statements about the effect of the instrument function on the Compton profile since it depends critically on both the shape and width of the function and on the shape of the profile. From reference to Table 4, however, it can be seen that a Gaussian instrument function of FWHM = 0·2 a.u. changes the renormalized value of $J(0)$ for water by 0·6%. For the X-ray experiments therefore, the deconvolution should present no problem since even without any deconvolution at all the error in $J(0)$ should only be of the order of 1·5%. For the γ-ray experiments the situation is somewhat worse.

There is however one aspect of deconvolution which has been almost completely ignored in nearly every paper in the literature concerned with Compton scattering. Paatero, Manninen & Paakkari (1974) have shown that even for an 'ideal' deconvolution procedure there will always be a 'residual instrument function' and a full statement of the results includes a statement of this function. (The easiest way to visualize the residual instrument function is to consider that function which would be obtained, after deconvolution, if the apparatus were set to measure a spectral line which was in reality a delta-function.) The reason for the importance of the residual instrument function is that a 'true' comparison can only be made between a theoretical profile, say, and an experimental profile if the theoretical profile is first convoluted with the residual instrument function. Fortunately, for a 'well behaved' profile like that of water, with no discontinuities in the profile or its first derivative, the effect of the residual instrument function should be fairly small. Further discussion of this point will be given in § 8.

In the γ-ray experiments the instrument function usually has a tail on the low-energy side which is very much smaller than the rest of the instrument function but often extends over a fairly large energy range. This can easily be allowed for by using a 'tail-stripping' procedure. The presence of such a tail in the instrument function also destroys the symmetry of the Compton profile about $p=0$.

7.7 *Multiple scattering*

The last and probably the most troublesome of the corrections is the correction to allow for the contribution to the observed spectrum from events involving more than one photon–electron scattering.

Unfortunately, the theory of multiple scattering in the Compton effect is still in its infancy, the only theoretical investigations of multiple scattering being by DuMond (1930) and Williams, Pattison & Cooper (1974). In the meantime the best that can be done is to summarize the current state of the theory.

7.7.1 *Dependence of multiple scattering on the cross section*

DuMond (1930) has shown that in the non-relativistic limit the ratio of double to single scattering should be proportional to the scattering cross section provided that there is no significant absorption in the sample. From tabulated values of the cross section (Storm, Gilbert & Israel, 1958) it is found that between 160 and 60 keV the cross section for water changes from 0·12 to 0·17 cm^2/g so that on this basis the fraction of double scattering from a given thin sample should be the same for Am as it is for Te γ-rays. For 15 keV incident photons, however, the cross section increases to 0·31 cm^2/g so that one might expect the ratio of double scattering to single scattering to be about twice as great in the X-ray experiments as in the γ-ray experiments.

7.7.2 *Dependence of multiple scattering on the sample thickness*

From DuMond's early theoretical work (DuMond, 1930) it can be seen that to a first approximation the fraction of double scattering in a Compton experiment varies as the average value of $1/r^2$ where r is the distance between any two points in the sample. (This is because the intensity of the intermediate ray goes as $1/r^2$ if it is assumed that the first scattering is isotropic and that there is no absorption.) Using this simple approximation one can show that the ratio of double to single scattering will vary as illustrated in Fig. 3 (Williams & Halonen, 1975). That is, for thin samples the ratio should vary linearly with the thickness, when the diameter and the length are approximately equal the ratio should be a maximum and for very thick samples the ratio should vary as the reciprocal of the thickness. These simple arguments indicate that in order to cut down the double scattering the sample thickness should be significantly less than the diameter and that a linear extrapolation to zero thickness is only valid for very thin samples.

7.7.3 *Spectral distribution of double scattering*

Williams, Pattison & Cooper (1974) have shown that if (*a*) the scattering angle is 180°, (*b*) $\Delta\lambda \ll \lambda_0$, and (*c*) the 'true' Compton profile is Gaussian, then the profile due to twice inelastically scattered radiation is identical to the single scattered profile. From these results it would seem that in order to minimize the multiple scattering the highest possible scattering angle should be used. In addition, for X-ray experiments at high angles, the effect of double scattering might be considerably less than expected on the basis of the total fraction of double scattering. (Note that this argument does not hold for once elastic, once inelastic double-scattered radiation, as shown by Williams *et al.*, 1974.)

7.7.4 *Fraction of double scattering*

Finally, it is worth noting that DuMond (1930) has shown that for a 1 cm diameter sphere of graphite and Mo $K\alpha$ radiation, the ratio of double scattering to single scattering should be about 14%. For water, therefore, for which the density is one third of that of graphite, the fraction of double scattering in a 1 cm diameter sphere might be expected to be of the order of 5%.

8. Reexamination of the data

Now that the collection and processing of Compton scattering data have been considered in detail, the results of the various measurements can now be reconsidered.

8.1 *Accuracy and resolution parameters*

Table 9 gives accuracy and resolution parameters for the data submitted by the various participants. As is expected, the resolution function is narrowest for the two X-ray experiments (1 and 5), followed by the Te γ-ray experiment (3), one of the Am γ-ray experiments (4) and then the other γ-ray experiment (2). The widest resolution function is about 2·5 times as wide as the narrowest. The statistical accuracy of the results varies by a factor of about five from data set 3 to set 4. However, a crucial feature which is not reflected in these figures is the effect of the deconvolution procedure on the experimental errors. An optimized deconvolution procedure might easily give an answer which is an order of magnitude more accurate than a poorly optimized procedure. Indeed, from the results of Cheng, Williams & Cooper, (1971) it follows that the statistical error on the final profile is inversely proportional to the width of the residual instrument function as defined by Paatero *et al.* (1974). There is therefore a degree of subjectivity in the choice of the residual instrument function and hence the error on the final data.

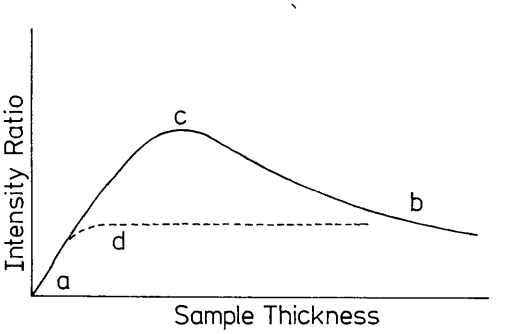

Fig. 3. The dependence of the ratio of double to single scattering on sample thickness. The solid line is a schematic representation for a sample with no absorption. For very thin samples the ratio increases linearly (*a*), for very thick samples the ratio varies inversely with the thickness (*b*), and the ratio is a maximum when the length and diameter of the sample are approximately equal (*c*). For a sample with absorption, there will be an upper limit to the effective sample thickness leading to the situation indicated by the dashed line (*d*).

Table 9. *Accuracy and resolution parameters for the project data*

The error is expressed as a percentage per 0·01 a.u. of momentum. Resolution 1 is the estimated FWHM of the apparatus function, resolution 2 is the estimated FWHM of the effective incident-beam (and scattered-beam) divergence function and resolution 3 is the α_1–α_2 spacing. All resolution parameters are expressed in atomic units. Resolution T is the total resolution parameter as defined in § 7·6.

Data set	1	2	3	4	5
Statistical error	0·7	0·9	0·3	1·4	1·3
Resolution 1	0·25	0·77	0·46	0·56	0·30
2	0·05	0·20	?	0·13	0·04
3	0·44	—	—	—	0·44
T	0·33	0·80	0·46	0·58	0·37

8.2 *Dependence of the profile shape on the sample thickness*

As was pointed out in § 7.7, the theory of the effect of multiple scattering on Compton profiles is still in its infancy, although this situation should soon be considerably improved. Apart from rather general theoretical statements therefore, the best approach is probably to measure a set of profiles for samples of varying thickness (or pressure, if a gas) and try to estimate the profile corresponding to zero thickness (or pressure). Fig. 4 shows the difference between the measurements of each data set and the thinnest sample from that set. The general form of the difference curves is very similar in all cases. The most important feature however is that all the difference curves have a maximum at about 2·0 a.u. so that it should be possible to distinguish between an error due to multiple scattering and any one of the other systematic errors illustrated in Fig. 2 which all peak at about 1·0 a.u. From Fig. 4(*c*) it is also clear that if the profiles are normalized to have the same area a linear extrapolation to zero thickness is not appropriate for small values of p. Using only the values near $p=0$, the best results would appear to correspond to an interpolation which goes as the square root of the thickness. However, for values of p between 3 and 4 a.u., the form of the extrapolation changes.

8.3 *General observations*

In Fig. 1 profiles 3, 4 and 5 are very close to one another (except at $p=0$), profile 1 is somewhat wider and profile 2 is wider still. The difference between the mean of profiles 3, 4 and 5 and profile 1 peaks around 1 a.u. and is negligible at and above 2 a.u. This indicates that the difference is due to a 'linear', 'scale' or 'shift' error rather than a 'background' error or the presence of multiple scattering in the data. Comparing the mean of profiles 3, 4 and 5 with profile 2 it is seen that the difference is negligible at 1·0 a.u. and peaks at about 2·0 a.u. This indicates that the difference is due mainly to the presence of multiple scattering in data set 2, which might be expected since the thinnest sample in this

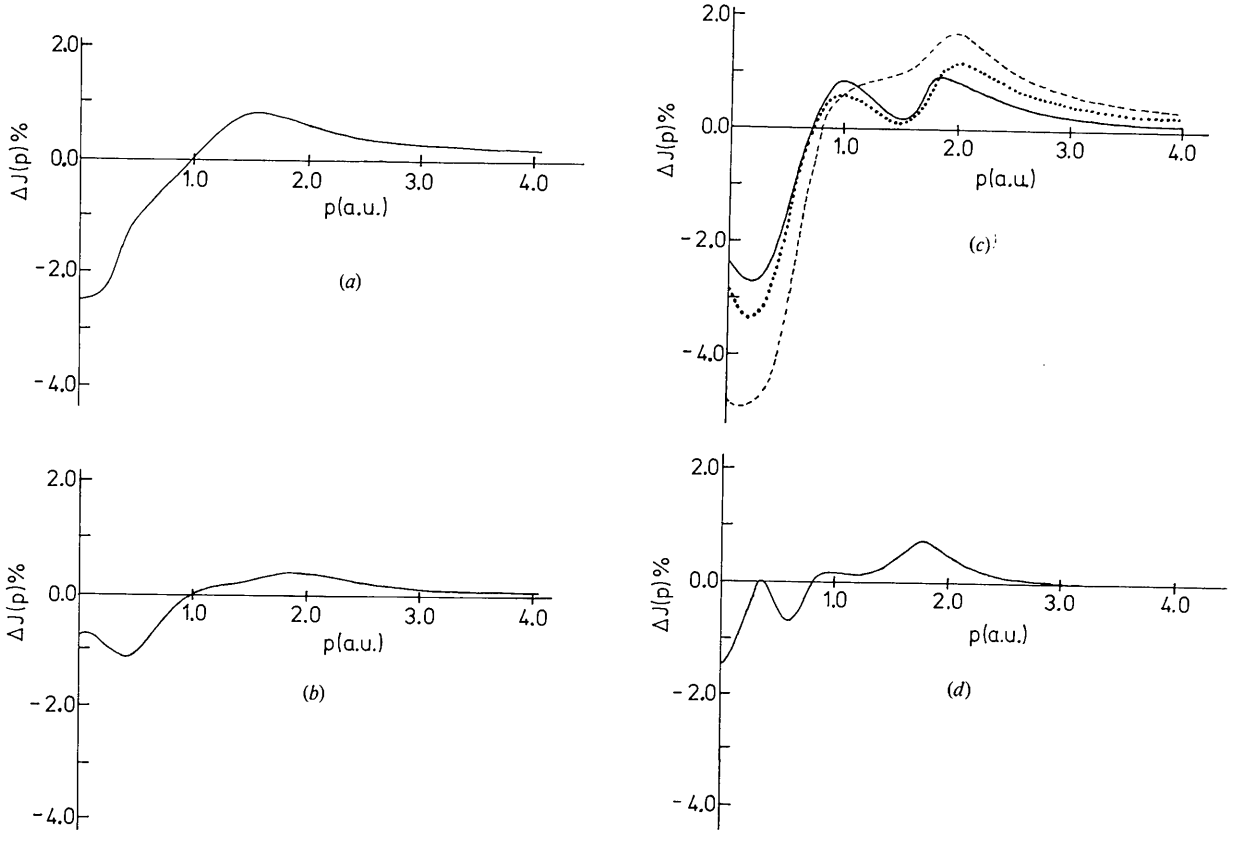

Fig. 4. The effect of sample thickness on the Compton profiles. For each data set the differences are plotted between each measurement and the measurement on the thinnest sample of that set. (*a*) Data set 2, (*b*) data set 3, (*c*) data set 4, (*d*) data set 5.

data set was 1 cm thick compared to 1 mm for set 4, 3 mm for sets 3 and 5 and 1·5 mm for set 1.

9. Examination of individual data sets

In this section the individual measurements will be discussed briefly, in the light of the discussion of §8, with a view to determining the most probable sources of error in each measurement.

9.1 *Data set* 1

The measurements referred to as data set 1 were taken with Ag $K\alpha$ fluorescence X-rays and a crystal spectrometer.

In this experiment, fluctuations in the intensity of the incident beam were allowed for by taking six separate measurements of the Compton profile. The accuracy of the gearing on the spectrometer was not recorded but it is unlikely that a standard crystal spectrometer would have errors in its gearing great enough to cause appreciable errors.

The signal-to-noise ratio was 11 to 1 which is good for an X-ray experiment but could still cause difficulties in the background subtraction. However, the tails of the profile shown in Fig. 1 agree well with the average value of the tails of the other measurements so that the background is probably quite accurate. The contributions from air scattering and from the foils of the container were measured but reckoned to be negligible.

As is expected in an X-ray measurement the correction for the wavelength dependence of the absorption in the sample and the detecting system is large, the value of the parameter λ in equation (1) being about 0·04 a.u.$^{-1}$. An error in the value of λ of 0·01 a.u.$^{-1}$ would change the value of $J(0)$ by about 1 % so that the absorption correction is a possible source of error.

The next potential error source is in the determination of the position of the Compton peak. Unfortunately, it was not stated if the scattering angle was used to calculate the peak position or if the centre of the profile was determined from the data. If the former course was adopted the scattering angle should have been determined to within 0·15° so that this could easily alter the final profile significantly. If the latter course of action was adopted the Bragg angle corresponding to the peak shift should be determined to within about 0·001° 2θ. Because of the rather strict requirements on the accuracy of the peak shift it would appear that this is a possible source of error. It should be noted that the form of the peak-shift error (Fig. 2) is quite similar to the difference between data set 1 and the mean of the other measurements (Fig. 1).

No details were given concerning the expression for the scattering cross section. Provided either the correct relativistic or non-relativistic expression was used this should not introduce any error. The correction for the non-linearity of the conversion from Bragg angles 2θ to energies of the scattered photon (§ 7·5) does appear to have been omitted. This would change the value of $J(0)$ by about 2 %.

This data was not deconvoluted to allow for the effect of the apparatus function although the α_1–α_2 separation was carried out. This data set does in fact have the narrowest total resolution function. However, from Table 5 it is seen that a Gaussian apparatus function of FWHM = 0·3 a.u. will give rise to a 1 % error in $J(0)$, so that the apparatus function for this data set, which has a FWHM = 0·25 a.u., might make a significant difference to the profile. If a correction for the deconvolution were included this would change the profile in the direction of the mean of the other profiles.

The last potential error source in this data set arises from the possibility of multiple scattering. However, the measurement was carried out on a 1·5 mm thick sample so that the effect of multiple scattering is likely to be small.

The error parameter for this data set compares very well with the other sets (Table 9).

Unfortunately no mention was made of the symmetry of the final profile. As has been pointed out above, this would provide a useful check on several of the possible sources of error.

9·2 *Data set* 2

The measurements referred to as data set 2 were taken using Am γ-rays and a solid-state detector.

The stability of the energy scale in this experiment was better than 19 eV which is quite adequate for these measurements.

Since this was a γ-ray experiment the background should not give rise to any difficulty. A separate measurement was carried out to determine the contribution from the air and the container.

No correction was applied to allow for the energy dependence of the absorption in the sample on the grounds that, if the data is extrapolated to zero thickness, no correction is necessary. Although this argument may not be valid, an estimate of the correction for a 1 cm thick sample of water gives a value for the parameter γ in equation (1) of 0·002 a.u.$^{-1}$ so that this correction would only change the value of $J(0)$ by 0·2 %.

The determination of the position of the Compton peak is again a possible source of error. For Am γ-rays the scattering angle should be determined to within 0·04° if it is to be used to determine the position of the Compton peak. If the data are used the centre of the profile should be estimated to within 12 eV. The accuracy with which the peak shift was determined was not specified so that this could affect the results significantly.

The non-relativistic expression was used for the cross section but this should not introduce any significant error.

This data set has the widest resolution function (FWHM = 0·8 a.u.) so that the deconvolution is particularly crucial. However, provided care is taken with the deconvolution the residual instrument function should not affect the profile significantly.

The most severe problem in this data set is that of multiple scattering since the thinnest sample for which a measurement was made was 1 cm thick. Indeed, if it is assumed that the arguments of § 7.7.2 are valid to a first approximation, then a linear extrapolation to zero thickness will almost certainly underestimate the amount of multiple scattering. Furthermore, the difference between data set 2 and the mean of the other measurements (Fig. 1) is very similar in shape to the differences between thick and thin sample measurements illustrated in Fig. 4. It is almost certainly true therefore that most, if not all, of the difference between data set 2 and the other measurements can be attributed to the presence of multiple scattering.

The error parameter for this data set compares favourably with the other sets (Table 9).

Again, no mention was made of the symmetry of the final profile. As has been pointed out, this would provide a useful check on several of the error sources.

9.3 *Data set* 3

The measurements referred to as data set 3 were taken using Te γ-rays and a solid-state detector.

No mention was made of the stability of the energy scale but with reasonably good equipment this should not cause any difficulties.

Since this was a γ-ray experiment the background should be almost negligible. To eliminate the contribution from the air, the mylar foils and the shielding, the multichannel analyser was set in the subtract mode and the experiment was run with the sample container empty for the same length of time as the original experiment.

No details were given of the momentum dependence of the absorption correction. However, an estimate of the correction for a 3 mm thick sample of water gives a value of the parameter λ in equation (1) of about 0·0002 a.u.$^{-1}$ so that the absorption of γ-rays in the sample should not affect the final profile. A more serious problem for Te γ-rays might be the variation of the detector efficiency with energy.

As in the two previous data sets, the determination of the position of the Compton peak is of crucial importance. The data were used to determine the centre of the profile to within 24 eV. This will not introduce any significant error.

The relativistic expression for the scattering cross section [equation (A10)] was used to correct the data.

The resolution function for this data set is reasonably narrow (FWHM = 0·46 a.u.) and a well optimized method was used for the deconvolution procedure. This is not likely therefore to introduce any error.

The thinnest sample used in this data set was 3 mm thick. However, from Fig. 4(*c*) it appears that for Am γ-rays the difference between the profiles measured for a 3 mm thick sample and a 1 mm. thick sample is still quite considerable (approximately 2% at the origin). The possibility of a significant contribution from multiple-scattering events cannot therefore be ruled out.

The error parameter shows that this is in fact the most accurate (in terms of the raw data) measurement of the project.

As in the previous two data sets, no mention was made of the symmetry of the final profile.

In this data set the tails of the Compton profile were measured out to 15 a.u. and it is worth noting the excellent agreement between these measurements and the tails of the NHF profile in Table 1.

9.4 *Data set* 4

The measurements referred to as data set 4 were taken using Am γ-rays and a solid-state detector.

The stability of the energy scale of the detecting system was checked several times during the course of the experiment by measuring the position of the line emitted from a weak Am test source. The energy scale was stable to within less than 12 eV throughout the experiment.

The signal-to-noise ratio was 500 to 1 and a linear background was subtracted. In order to minimize the scattering from the lead shielding, the experiment was arranged in such a way that no part of the shielding was in direct line with both the incident and scattered beams. This technique requires the use of a somewhat lower scattering angle and consequently tighter collimation on the incident and scattered beams. A separate measurement was made with the sample container empty to allow for the contribution from the foils on the container. This contribution was particularly large for the measurement on the 1 mm sample but will only increase the random errors and should not introduce any systematic error.

The correction for absorption in the sample was very small, the value of the parameter λ in equation (1) being 0·0002 a.u.$^{-1}$ so that this will not cause any significant problem. No correction was applied for the variation of the detector efficiency with energy but for Am γ-rays this problem should not be too serious.

The peak shift of the profile was determined by fitting a parabola to the central part of the curve. In this way the peak shift was determined to within less than 12 eV so that this will not introduce any significant systematic error.

The relativistic expression for the scattering cross section [equation (A10)] was used to correct the data. However, the correction for the non-linearity of the conversion to momentum units was then incorrectly applied again, as discussed in § 7.5. This will cause an error of about 1·2% in $J(0)$.

The resolution function for this data set was rather wider than some of the others (FWHM = 0·58 a.u.) but the deconvolution procedure is very well optimized and the residual instrument function is unlikely to alter the results significantly.

The contribution from multiple-scattering events should be very small in this data set since a measurement was carried out on a sample of 1 mm thickness. In addition, the fact that measurements were made on four sample thicknesses should provide a good check on multiple scattering when the theory of multiple scattering is developed further.

The accuracy of the raw data in this experiment is lower than some of the others but this is probably made up for by using a very carefully optimized deconvolution procedure.

In order to check the symmetry of the final profile the area under the curve was calculated for each experiment between -7 and 0 a.u. and between 0 and $+7$ a.u. From the values of these integrals given in Table 10 it is seen that the difference in the areas as a percentage of the area is about 1% for the three thinnest samples. This implies that the total error in $J(0)$ due to errors in the absorption correction, the peak shift and the cross-section correction is unlikely to be more than 0·5%. The large difference for the 16 mm thick sample is probably due to the presence of multiple scattering in that experiment.

Table 10. *Asymmetry in the Compton profiles of data set* 4

A is the integral from -7 to 0 a.u., B the integral from 0 to $+7$ a.u. Δ is the difference between A and B and % is Δ expressed as a percentage of the mean of A and B.

Thickness (mm)	A	B	Δ	%
16	3·533	3·453	0·08	2·3
6	3·612	3·584	0·03	0·9
3	3·629	3·580	0·05	1·4
1	3·720	3·680	0·04	1·2

9.5 *Data set* 5

The measurements referred to as data set 5 were taken using Mo $K\alpha$ fluorescence X-rays and a crystal spectrometer.

The stability of the incident X-ray beam was checked to within 0·5% and in addition the final profiles were the mean of five separate measurements. By measuring a series of fluorescence lines as well as the straight through beam the gears were found to be accurate to within 0·002° 2θ between 0° and 60° of 2θ.

The background was subtracted by drawing a straight line through points at about 35·00° 2θ (beyond the β lines) and 50·60° (in the tail of the α profile). With this background it was found that the measured profile differed significantly from the NHF profile (Table 1) in the tails. Consequently, the experimental profile was matched to the NHF profile at 9 a.u. of momentum on the long-wavelength side.

In order to minimize the scattering from the lead shielding, the 'cross-over' technique described in § 9.4 was used. A separate measurement was made with the sample container empty to allow for the contribution from air scattering and from the foils on the container.

Since this was an X-ray experiment the absorption correction must have been quite large. No details were given as to the size of the absorption correction but the final profile was calculated as the average of the short- and long-wavelength sides. Consequently, any error in the absorption correction should cancel. (The average was of course only taken up to the absorption edge.)

After the separation of the α_1 and α_2 components by the method of Rachinger, the position of the Compton peak was determined by fitting a parabola to the central part of the curve. In addition, the fact that the final profile was given as the average of the long- and short-wavelength sides of the profile should eliminate any small error arising from an incorrect determination of the peak shift.

The non-relativistic expression was used for the scattering cross section but this should not introduce any error. The correction for the non-linearity of the conversion from Bragg angles to momentum was not included. However, any error introduced as a result will cancel when the sides of the profile are averaged.

Since this was an X-ray measurement the resolution function was fairly narrow. In addition a well optimized deconvolution procedure was used so that it is unlikely that the residual instrument function will affect the result significantly.

The thinnest sample used in this data set was 3 mm thick so that as for data set 3 there is the possibility that the results could be affected by multiple scattering events.

The accuracy of the raw data in this experiment is lower than some of the others but this might be compensated for to some extent by the use of a well optimized deconvolution procedure.

10. Conclusions

From the results described above, and in particular from Fig. 1, it would seem that Compton profiles can easily be measured with a reproducibility of ±2%. In addition, if experiments are done very carefully on thin samples (or if a gas, at low pressures) a reproducibility of ±1% is not an unreasonable expectation. In a differential experiment, such as a measurement on two geometrically identical crystals differing only in the orientation of the crystal lattices, a reproducibility of ±0·5% should be possible.

The most important unresolved problem is the question of how multiple-scattering events affect the profile shape. However, multiple scattering of X-rays is well understood in principle and it is only necessary to set up computer programs to calculate or correct for this effect. There are three possible approaches to this problem. Firstly, one can minimize the amount of multiple scattering in the sample by using as thin a sample as possible (or in the case of a gas as low a pressure as possible). Secondly, one can eliminate the single scattering and measure only the multiple scattering using the displaced beam technique (Philips & Chin, 1973) and then use this to correct the observed profile. Finally, it should be possible to calculate the spectral distribution of the multiple-scattering events (probably using Monte Carlo techniques) and use this to correct measurements on thick samples. Combinations of these approaches should lead to a good understanding of multiple scattering in the near future.

Apart from multiple scattering the most crucial error source is the determination of the peak shift. The problem is that a very small error in the peak shift gives rise to a substantial error in the area so that the value of $J(0)$, after renormalization, may change considerably.

Finally, the correction to allow for the energy dependence of the detector efficiency has been ignored in the experiments using X-rays and Am γ-rays. Although this correction is only likely to be significant for Te γ-rays, measurements should be done in the energy region of Am γ-rays to ensure that it is negligible for these experiments.

At this stage of the project it is probably not wise to try and estimate the 'true' profile. However, the mean of the data in Fig. 1, excluding data set 2 for which the multiple scattering contribution is large, is probably a reasonable estimate with the proviso that the 'true' curve is almost certainly somewhat narrower than this.

11. Proposals

In order to obtain more consistent data in the future the following recommendations are made.

11.1 *Normalization*

When Compton profile measurements are reported, it is important to state

(*a*) the range (in a.u.) over which the profile was normalized,

(*b*) the value taken for this area (usually the Hartree–Fock free-atom area),

(*c*) the interpolation intervals used in the integration.

11.2 *Symmetry*

The symmetry of the final profile should be clearly stated as this provides a useful check on many error sources. (This may not always be possible if binding edges occur in the region of interest).

11.3 *Analytical corrections*

Details of all the corrections should be given. For example, the value of the parameter λ in equation (1) corresponding to the absorption correction, the cross-section correction and the correction for the non-linearity of the conversion to the momentum scale should be stated.

11.4 *Numerical corrections*

The residual instrument function should be stated. Although this does not appear to affect any of the water profiles significantly, for profiles which have a discontinuity in the first derivative (such as the profiles of metals or for particularly narrow profiles) this function might be of crucial importance.

11.5 *Accuracy and resolution*

All experimental results should include a precise statement of the accuracy and resolution parameters, preferably in the form used in Table 10.

11.6 *Geometry*

Full details of the scattering geometry should be given. If it proves to be possible to compute the spectral distribution of the multiple scattering it will probably be necessary to know the scattering angle, sample thickness, the illuminated volume of the sample and so on. The importance of specifying precisely the scattering geometry cannot, therefore, be overstressed.

The work and ideas discussed in this report are due to Pentti Paatero, Seppo Manninen, Timo Paakkari, Vesa Halonen, Peter Eisenberger, Irving Epstein, Richard Weiss, William Reed, Brian Williams, Johsua Felsteiner, Malcolm Cooper and Philip Pattison.

I would like to thank the Royal Society for the award of an Overseas Fellowship during the tenure of which I was able to collate this information. I would also like to thank the many friends at the University of Helsinki who helped and encouraged me in this work. Finally, the IUCr *Ad-Interim* Commission on Spin, Charge and Momentum Density and in particular Dr Richard Weiss deserve special thanks for providing the encouragement and incentive which made this all possible.

APPENDIX I

1. The error in the peak shift of the Compton profile due to an error in the energy scale

The relation between the momentum of the scattering electron and the energies of the incident and scattered photons is

$$p=\frac{\gamma(w_1-w_2)-w_1w_2(1-\cos\varphi)}{[w_1^2+w_2^2-2w_1w_2\cos\varphi]^{1/2}} \qquad \gamma=1+p^2/2 \tag{A1}$$

where p is the z component of the momentum of the scattering electron in units of mc, w_1 and w_2 are the energies of the incident and scattered photons in units of mc^2, φ is the scattering angle and γ the relativistic energy of the scattering electron, and

$$p\simeq\frac{w_1-w_2-w_1w_2(1-\cos\varphi)}{[w_1^2+w_2^2-2w_1w_2\cos\varphi]^{1/2}}\ . \tag{A2}$$

From (A2) it follows that

$$\left.\frac{\partial p}{\partial w_2}\right|_{p=0}=-\frac{1+w_1(1-\cos\varphi)}{[w_1^2+w_2^2-2w_1w_2\cos\varphi]^{1/2}} \tag{A3}$$

and at $p=0$

$$w_2=\frac{w_1}{1+w_1(1-\cos\varphi)}\ . \tag{A4}$$

Table 11 gives values of $\partial p/\partial w_2|_{p=0}$ for a range of values of w_1 and φ.

Table 11. *The error in the peak shift of the Compton profile due to an error in the energy scale* (a.u./keV)

	Scattering angle		
E_0 (keV)	100°	140°	180°
160	0·88	0·86	0·86
60	1·80	1·60	1·56

2. The error in the peak shift of the Compton profile due to an error in the Bragg angles

$$\left.\frac{\partial p}{\partial 2\theta}\right|_{p=0}=\frac{\partial p}{\partial w_2}\frac{\partial w_2}{\partial\lambda_2}\frac{\partial\lambda_2}{\partial 2\theta}\Bigg|_{p=0} \tag{A5}$$

$$\frac{\partial w_2}{\partial\lambda_2}=-w_2^2=\frac{-w_1^2}{[1+w_1(1-\cos\varphi)]^2} \tag{A6}$$

$$\frac{\partial\lambda_2}{\partial 2\theta}=\frac{d}{n}\cos\theta\ . \tag{A7}$$

Table 12 gives values of $\partial p/\partial 2\theta|_{p=0}$ for 20 keV photons, $n=4$, $d=4{\cdot}0267$ (LiF) and a range of values of φ.

Table 12. *The error in the peak shift of the Compton profile due to an error in the Bragg angles* (a.u./deg. 2θ)

	Scattering angle		
E_0 (keV)	100°	140°	180°
20	2·35	1·89	1·77

3. The error in the peak shift of the Compton profile due to an error in the scattering angle

$$\left.\frac{\partial p}{\partial\varphi}\right|_{p=0}=\frac{\partial p}{\partial w_2}\frac{\partial w_2}{\partial\varphi}\Bigg|_{p=0} \tag{A8}$$

$$\left.\frac{\partial w_2}{\partial\varphi}\right|_{p=0}=\frac{-w_1^2\sin\varphi}{[1+w_1(1-\cos\varphi)]^2}\ . \tag{A9}$$

Table 7 gives values of $\partial p/\partial\varphi|_{p=0}$ for a range of values of w_1 and φ.

APPENDIX II

1. Momentum dependence of the scattering cross section

The differential cross section for scattering through 180° is (Manninen, Paakkari & Kajantie, 1974)

$$\frac{d^2\sigma}{d\omega_2 d\Omega}\sim\frac{w_2}{w_1}\frac{\frac{w_1A_1}{w_2A_2}+\frac{w_2A_2}{w_1A_1}+\frac{4}{(A_1A_2)^2}[1-A_1A_2]}{(w_1A_1+w_2A_2)} \qquad A_1=1+p,\quad A_2=1-p\ , \tag{A10}$$

where p is the momentum of the scattering electron in units of mc of momentum and w_1 and w_2 the energies of the incident and scattered photons, respectively, in units of mc^2.

Using (A2) with $\varphi=180°$ to eliminate w_2 and keeping only terms up to first order in p, (A10) reduces to

$$\frac{d^2\sigma}{dw_2 d\Omega}\sim\frac{1}{w}\left(\frac{2w^2+2w+1}{2w^2+3w+1}\right)\times\left[1-\left(\frac{4w^4+12w^3+10w^2+4w+1}{4w^4+10w^3+10w^2+5w+1}\right)p\right] \tag{A11}$$

$$(w\equiv w_1)$$

$$=\frac{1}{w}N[1-\lambda p]\ ,$$

where N is always between 0·8 and 1 and λ is always between 0·94 and 1·04.

Considering now the non-relativistic expression gives

$$\frac{d^2\sigma}{dw_2 d\Omega} \sim \frac{w_2}{w_1(w_1+w_2)} \tag{A12}$$

from which it follows that

$$\frac{d^2\sigma}{dw_2 d\Omega} \sim \frac{1}{w}\frac{1}{a+w}[1-p]\,. \tag{A13}$$

From (A11) and (A13) it follows that the non-relativistic expression for the momentum dependence of the cross section is not significantly different from the relativistic expression and the momentum dependence can be taken as $1-p$ or if p is in a.u.

$$\frac{d^2\sigma}{dw_2 d\Omega} \sim 1-0{\cdot}007p\,. \tag{A14}$$

2. Non-linearity of the conversion from Bragg angles to momentum units

When the Bragg angles are converted to energy units the identity

$$J(w_2)dw_2 = J(2\theta)d2\theta \tag{A15}$$

should be borne in mind.

From the equation relating the wavelength (λ_2) of the scattered photon to its energy (w_2) it follows that

$$\frac{dw_2}{d\lambda_2} \sim -w_2^2\,. \tag{A16}$$

Using (A1) with $\varphi = 180°$ to express (A16) in terms of p,

$$\frac{dw_2}{d\lambda_2} \sim 1-4p \tag{A17}$$

with p in units of mc.

Now using Bragg's law, *viz.*

$$n\lambda_2 = 2d\sin\theta\,, \tag{A18}$$

where n is the order of the reflexion from an analysing crystal for which the lattice spacing is d, it follows that

$$\frac{d2\theta}{d\lambda_2} \sim 1-\lambda p\,,$$

with

$$\lambda = \frac{2n^2(\lambda_1+\lambda_c)(\lambda_1+2\lambda_c)}{(2d)^2-n^2(\lambda_1+2\lambda_c)^2}\,, \tag{A19}$$

provided $p \ll 1$ (note that λ should not be confused with λ_1, λ_2 and λ_c representing wavelengths).

Using (A17) and (A18) to evaluate $d2\theta/dw_2$ for 20 keV photons analysed with a LiF crystal in the 400 reflexion,

$$\frac{d2\theta}{dw_2} \sim 1+0{\cdot}025p \text{ with } p \text{ in a.u.} \tag{A20}$$

Addendum. Since this report was written, Felsteiner, Pattison & Cooper (1974) have calculated the intensity and spectral distribution of double and triple scattering. They used this calculation to correct profiles 2*A* and 2*C* for the effect of multiple scattering. Their results show that most of the difference between data set 2 and the mean of the other results can be explained in terms of multiple scattering in agreement with the conclusions drawn in § 9.2.

References

Abrahams, S. C., Alexander, L. E., Furnas, T. C., Hamilton, W. C., Ladell, J., Okaya, Y., Young, R. A. & Zalkin, A. (1967). *Acta Cryst.* **22**, 1–6.

Abrahams, S. C., Hamilton, W. C. & Mathieson, A. McL. (1970). *Acta Cryst.* A**26**, 1–18.

Cheng, R. C. H., Williams, B. G. & Cooper, M. J. (1971). *Phil. Mag.* **23**, 115–133.

Cooper, M. J. (1971). *Advanc. Phys.* **20**, 453–491.

DuMond, J. W. M. (1930). *Phys. Rev.* **36**, 1685–1701.

Eisenberger, P. & Reed, W. A. (1972). *Phys. Rev.* A**5**, 2085–2094.

Eisenberger, P. & Reed, W. A. (1974). *Phys. Rev.* B**9**, 3237–3241.

Epstein, I. R. (1975). *M. T. P. Int. Rev. Sci. Phys. Chem. Ser.* II, edited by A. D. Buckingham.

Epstein, I. R. & Williams, B. G. (1973). *Phil. Mag.* **27**, 311–328.

Felsteiner, J., Pattison, P. & Cooper, M. J. (1974). *Phil. Mag.* **30**, 537–548.

Lloyd, K. H. (1969). *Amer. J. Phys.* **37**, 329–330.

Mackenzie, J. K. & Maslen, V. W. (1968). *Acta Cryst.* A **24**, 628–639.

Manninen, S., Paakkari, T. & Kajantie, K. (1974). *Phil. Mag.* **29**, 167–178.

Paakkari, T., Suortti, P. & Inkinen, O. (1970). *Ann. Acad. Sci. Fenn. A* **VI**, **345**, 1–28.

Paatero, P., Manninen, S. & Paakkari, T. (1974). *Phil. Mag.* **30**, 1281–1294.

Phillips, W. C. & Chin, K., (1973). *Phil. Mag.* **27**, 87–93.

Reed, W. A. & Eisenberger, P (1972). *Phys. Rev.* B**6**, 4596–4604.

Reed, W. A., Eisenberger, P., Pandey, K. C. & Snyder, L. C. (1974). *Phys. Rev.* B**10**, 1507–1515.

Storm, E., Gilbert, E. & Israel, H. (1958). *Gamma-ray Absorption Coefficients for Elements* 1 *through* 100, Nat. Tech. Info. Service, U.S. Dept. of Commerce, LA 2237.

Tanner, A. & Epstein, I. R., (1974). *J. Chem. Phys.* **61**, 4251–4257.

Viegele, W. J., Tracy, P. T. & Herny, E. M. (1969). *Amer. J. Phys.* **37**, 806–808.

Williams, B. G. & Halonen, V. (1975). *Phys. Fenn.* **10**, 5–20.

Williams, B. G., Pattison, P. & Cooper, M. J. (1974). *Phil. Mag.* **30**, 307–317.